

Efficient Design of Reinforced Columns: Insights into Lateral Confinement and Performance

Badhon Singha^{1*}, Nafis Niaz Chowdhury¹,
Mohammad Atiqur Rahman Sakib¹

¹Graduate Student, Ahsanullah University of Science and Technology,
Dhaka, 1215, Bangladesh

*Corresponding Author: badhon10776@gmail.com

(Received 10-11-2024; Revised 03-12-2024; Accepted 06-12-2024)

Abstract

In this research, the effects of hoop spacing on load-carrying capacity and deformation behaviour are examined in relation to the structural performance of reinforced concrete columns subjected to seismic strain rates. The study incorporates properties from analytical and experimental methods to simulate the stress-strain behaviour of constrained concrete using ABAQUS finite element modelling. To optimize hoop spacing, parametric research is carried out with the goal of balancing material cost and structural performance. To assess how different hoop spacing affects column performance, the load vs. displacement relationships is examined. The findings show that while optimal configurations improve load capacity and deformation resilience, excessive hoop spacing causes early spalling and decreased structural strength. This study contributes to safer and more effective structural systems by offering useful insights into the economical design of reinforced concrete columns with enhanced seismic performance.

Keywords: Confined concrete, Finite model, Lateral reinforcement, Mander model, and Unconfined concrete.

1 Introduction

A column, a fundamental vertical structural member in the realms of structural engineering and architecture, serves as the primary support for compressive loads. In the intricate fabric of a building or structure, columns play a multifaceted role with crucial functions such as load-bearing, providing support to horizontal components like beams and slabs, imparting height and stability, and facilitating the systematic distribution of loads to the foundation. The resistance of columns to compressive forces is paramount

for the overall stability and integrity of the structure, preventing any risk of structural failure.

Spiral columns, characterized by their cylindrical structure with continuous spiral bars, embody a specialized design with helical reinforcement. The helical reinforcement, also known as spiral reinforcement, contributes to transverse support, preventing lateral expansion of the concrete. Spiral columns, particularly suited for situations requiring flexibility or cost-effective enhanced strength under high loads, showcase the intricacies of structural engineering design.

On the other hand, tied columns, constituted by longitudinal bars connected by narrower bars at regular intervals, represent a predominant structural form in non-seismic locations. The ties, often transverse bars of smaller diameter, provide crucial lateral confinement, ensuring the verticality of longitudinal bars during construction and contributing to buckling resistance. The failure of a tied column leads to the crushing and shearing of concrete in all directions.

The focal point of this discourse extends to the behavior of reinforced concrete (RC) columns under lateral confinement, a critical consideration in earthquake-resistant design. The application of lateral confinement, achieved through confining reinforcement such as ties or spirals, is pivotal in understanding and enhancing the structural performance of columns, particularly in seismic regions.

Examining the relationship between force and displacement is foundational to comprehending structural behavior. Structural stiffness, a defining factor in how a structure or structural element deforms under applied force, plays a central role in ensuring safety and performance. The selected research on lateral confinement behavior in integrated concrete columns holds significant implications for determining load-carrying capacity, deformation behavior, and the application of the Mander model in both unconfined and confined concrete columns.

2 Background Studies

Numerous studies have explored the modeling of confined and unconfined concrete behavior, as well as the confinement effect in column strengthening. The schematic of concrete column shown in Fig. 1. The stress-strain relationship in concrete is well-

understood up to its maximum strength, but recent research has mainly focused on the post-peak phase and high-strength concrete characteristics. A key area of investigation is establishing an effective stress-strain relationship for confined concrete, achieved through strategic placement of transverse reinforcement. In low-stress conditions, transverse reinforcement experiences minimal strain, causing the concrete to behave similarly to unconfined concrete. As stress approaches the uniaxial strength, internal fracturing leads to dilation, resulting in a confining effect, which significantly enhances concrete strength and ductility.

Unconfined concrete

Kent and Park (1971) [1] proposed stress-strain equations for both confined and unconfined concrete, expanding upon Hognestad's (1951) [2] formulations to more comprehensively depict the post-peak stress-strain patterns. Subsequently, Popovics (1973) [3] introduced an equation designed to characterize the stress-strain behaviour specifically for unconfined concrete. Thorenfeldt et al. (1987) [4] later modified Popovics' (1973) [3] model to incorporate adjustments accounting for the descending branch of the specific stress-strain connection. Seeking enhanced control over the post-peak segment of the stress-strain relationship, Tsai (1988) [5] presented a generalized iteration of the Popovics (1973) [3] equation.

The evolution of these stress-strain equations reflects a progressive refinement in modeling concrete behaviour under various conditions. Kent and Park's (1971) [1] extension of Hognestad's (1951) [2] work suggests a desire for a more nuanced understanding of post-peak stress-strain phenomena. Popovics (1973) [3] contributes with a specialized equation catering to the unconfined concrete scenario, and subsequent modifications by Thorenfeldt et al. (1987) [4] address nuances in the descending branch of the specific stress-strain connection. Tsai's (1988) [5] generalized version further emphasizes the need for precise control over the post-peak behavior, underlining a continuous pursuit of accuracy and applicability in stress-strain modeling for concrete.

These developments, rooted in the pioneering work of Kent, Park, Hognestad, Popovics, Thorenfeldt, and Tsai, collectively advance the understanding of concrete behavior across various loading conditions. The iterative refinement of stress-strain equations contributes to the ongoing quest for comprehensive and accurate

representations of concrete response, essential in the field of structural engineering and materials science.

Confined concrete

The stress-strain model formulated by Kent and Park (1971) [1] underwent modifications, prompted by findings from Roy and Sozen's (1964) [6] tests on small square columns, which demonstrated the inefficacy of confinement by rectangular or square rings in appreciably increasing the compressive strength of concrete. Desayi et al. (1978) [7] addressed this by developing a unified equation-based stress-strain model, incorporating insights from tests conducted on circular columns with lateral spiral reinforcement, to elucidate both pre- and post-peak behavior of confined concrete.

Scott et al. (1982) [8] conducted a study involving square concrete columns, laterally braced by stacked arches and reinforced longitudinally, to explore the effects of lateral reinforcement configurations, especially under high strain rates common in seismic loading. Unlike the Kent and Park (1971) [1] model, calibrated for small-scale testing, Scott et al. (1982) [8] observed a significant increase in strength with robust confinement reinforcement. To accommodate this enhanced compressive strength at high strain rates, minor adjustments were made to the Kent and Park model.

Mander et al. (1988a) [9] expanded the scope by evaluating full-sized square, rectangular, and circular columns at seismic strain rates, investigating diverse lateral reinforcement configurations. Their subsequent model (Mander et al., 1988b) [10] incorporated a fracture criterion based on the five-parameter model of William and Warnke (1975) [11] combined with insights from Schickert and Winkler (1979) [12], resulting in a widely used, generalized multiaxial confinement model. However, the model exhibits limitations with the rise in usage of high-performance materials, necessitating potential revisions.

Yong et al. (1989) [13] proposed a stress-strain relationship specifically for linearly confined high-strength concrete, utilizing two polynomial equations defining the ascending and post-peak branches. Bjerkeli et al. (1990) [14] explored the ductility of high-strength, stress-resistant, reinforced concrete columns subjected to axial loads, identifying factors such as cross-section shape, reinforcement confinement ratio, and concrete compressive strength as key influencers in the stress-strain relationship. Li et al.

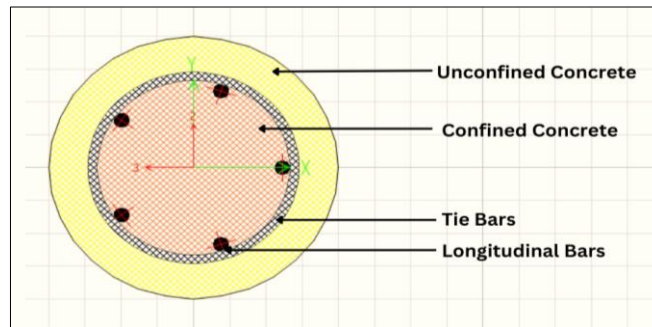


Figure 1. Specifications of concrete column

(2000) [15] conducted experimental tests on high-strength concrete columns confined by various transverse reinforcements, concluding that the stress-strain curve's shape is strongly influenced by confining reinforcement characteristics. Building upon this, Li et al. (2001) [16] developed a three-branch stress-strain model for high-strength concrete under normal- and high-yield-strength transverse reinforcement, based on their comprehensive experimental study. These sequential refinements underscore a continuous pursuit of precision and applicability in stress-strain modeling for confined concrete structures in the realm of structural engineering.

3 Analysis Methodology

The fundamental principle in ABAQUS is the step-by-step breakdown of issue history, where each useful period, encompassing dynamic transients, creep holds, or thermal transients, is denoted as a step. A step in ABAQUS/Standard may range from a basic static analysis of a load shift to more intricate scenarios.

In explicit dynamics processing, a multitude of tiny time increments is effectively executed using the explicit central-difference time integration method. Each increment, owing to the absence of simultaneous equation solutions, is relatively economical compared to the direct-integration dynamic analysis process in ABAQUS/Standard. The velocity and displacement solutions are advanced in time by utilizing accelerations

computed at time 't,' satisfying dynamic equilibrium equations through the explicit central-difference operator.

In the context of field output, ABAQUS/CAE permits the request of full sets of fundamental variables (e.g., components of strain or stress), showcased in X-Y data plots for reasonably frequent output requests in specific model areas.

The concept of embedded regions involves embedding model regions within their host regions or throughout the entire model using embedded region constraints. Here, reinforcement is embedded within the host region, which is concrete. Coupling constraints prove beneficial when a collection of coupling nodes is constrained to the rigid body motion of a single node. Such constraints find practical applications in providing model loads or boundary conditions. Two types of boundary conditions are employed, particularly for fixing one end of the column.

The analysis involves the utilization of six different models as listed in Table 1. each demonstrating significant differences as shown in Figs. 2-7. These differences primarily lie in the hoop distance or pitch distance between consecutive models. This approach allows for a comprehensive exploration of the impact of varying parameters on the structural behavior within the analytical framework.

Table 1. Description of the Models (for Abaqus FE analysis)

Model No.	Height (mm)	Diameter (mm)	Longitudinal Rebar length (mm)	Main Rebar	Hoop Size
1	2000	254	1898.4	5#5 bar	12#5 bar
2	2000	254	1898.4	5#5 bar	7#3 bar, 2#4 bar
3	2000	254	1898.4	5#5 bar	12#3 bar
4	2000	254	1898.4	5#5 bar	12#3 bar
5	2000	254	1898.4	5#5 bar	13#3 bar
6	2000	254	1898.4	5#5 bar	13#3 bar

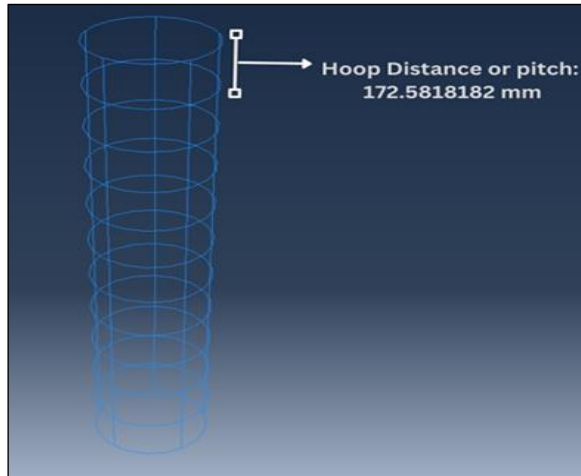


Figure 2. Model-1

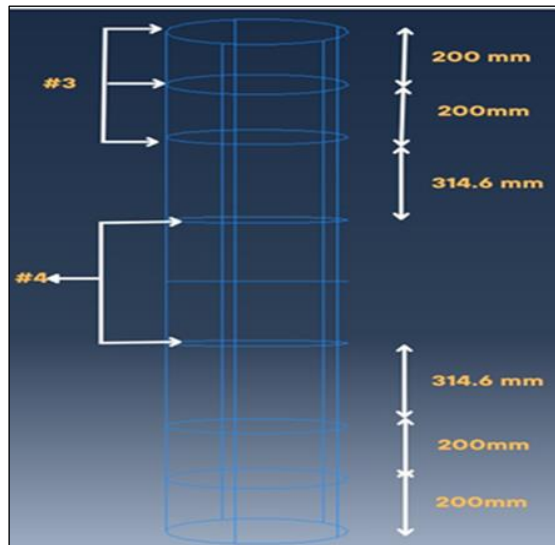


Figure 3. Model-2

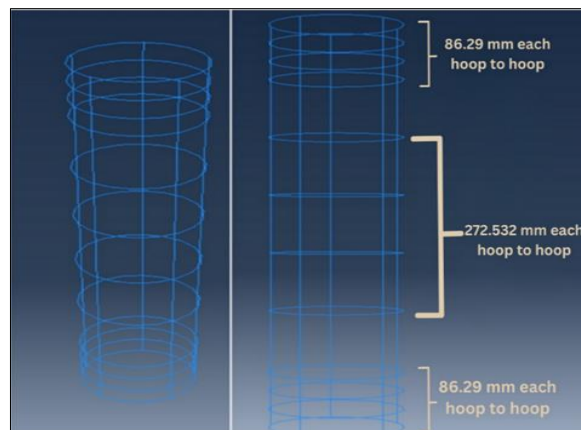


Figure 4. Model-3

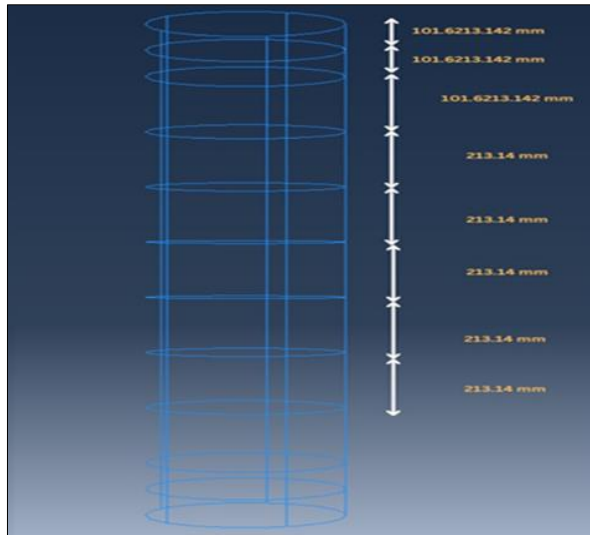


Figure 5. Model-4

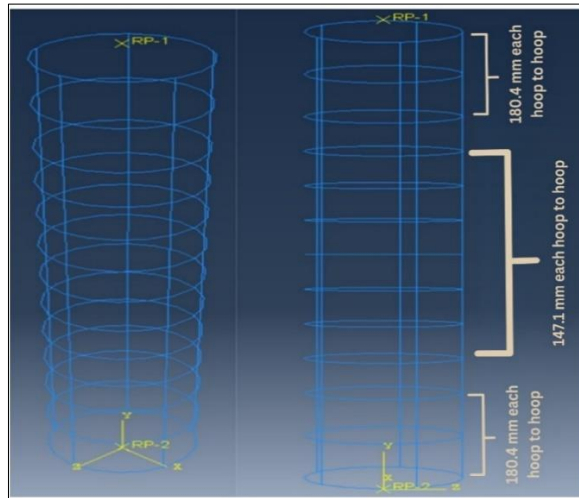


Figure 6. Model-5

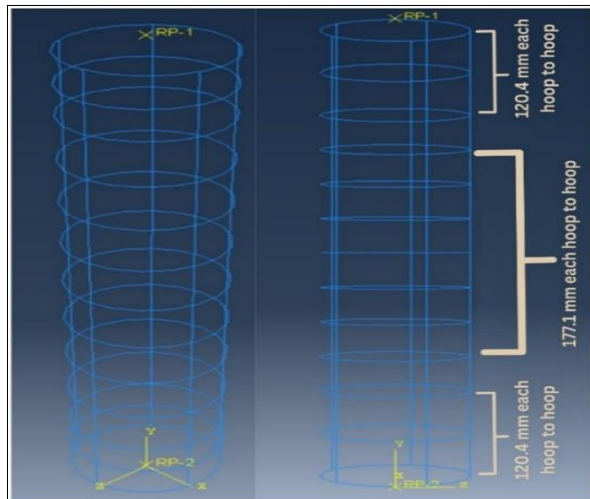


Figure 7. Model-6

4 Model Validation

The validation of the Abaqus model references the experimental work of Guadagnuolo et al. (2020) [17], focusing on concrete column behavior with varying transverse reinforcement details. The process involves defining input parameters like material properties, geometry, meshing, and loading conditions to mirror the experimental setup. Comprehensive data from the reference study, including dimensions, material properties, loading conditions, and force-displacement data, ensures accurate alignment with the physical model. The final model of concrete column shown in Fig. 8. Validation focuses on peak force values, disregarding post-ultimate force data. A rigorous comparison with a database of experimental and simulation results establishes the finite element (FE) model's reliability and accuracy for reinforced concrete columns.

The key material, as well as geometrical characteristics about the experimental data, has been summarized in Table 2. The column dimension of the reference work has been given in Table 2. The simulation in Abaqus produced a force vs. displacement graph, enabling a detailed comparison of the ultimate force obtained through finite element (FE) analysis with experimental results as shown in Fig. 9. The ultimate force from the FE analysis is 2953.03 kN, while the corresponding value from the reference experiment (Guadagnuolo et al. (2020) [17]) is 2990.09 kN. This comparison, conducted entirely through software simulation, shows a close agreement with a marginal difference of 1.24%, emphasizing the model's accuracy. The validation process in Abaqus involved replicating experimental setups, defining material properties, geometry, meshing, and

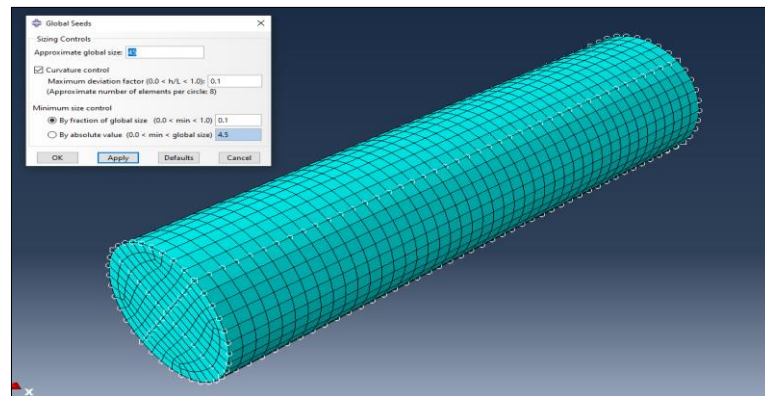
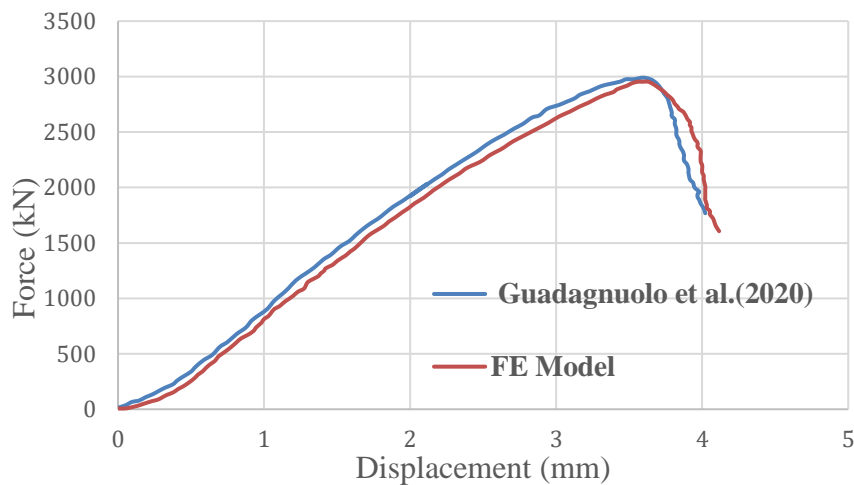


Figure 8. Fine meshing for FE simulation

Table 2. Reference and test specimen details

Research Name	Column Specimen	Concrete, f_{cu} (MPa)	Column dimensions (mm x mm x mm x mm)	Steel reinforcement long bars	f_y (MPa)		Hoop Size
					Long .Bars	Tie Bars	
Guadagnuolo et al. (2020)	Column-58	27.80	300 × 300 × 1300	8Φ12 mm	450	450	Φ8@150 mm

**Figure 9.** Force vs Displacement graph

loading conditions to ensure precise alignment. The close match between simulated and experimental results highlights the reliability of the FE model in capturing the structural response of reinforced concrete columns.

5 Results and Discussions

Finding the effectiveness of confinement in reinforced column:

This simulation in SAP 2000 for figure out the effectiveness of hoop distance in the column stress strain capacity. The hoop distance is decreased linearly in columns. Several Columns in different pitch conditions has been simulated in this research. At the end of the simulation, it has been seen that different models have different ultimate forces at

different displacements. The ultimate force that a column can bear is governed by a number of parameters, including its size, material qualities, and kind of loading. The diameter or hoop-to-hoop spacing of a column can impact its capacity to withstand axial loads (compression or tension), lateral loads (bending), and other forces. In general, increasing the diameter of a column while holding other elements constant improves the column's capacity to carry axial stresses and resist buckling.

A sample column has been Simulated on the SAP2000. Where are eight different pitch distances as listed in Table 3. For those, the different stress vs strain graphs have been found (shown in Fig. 10).

Table 3. Stress-Strain observation of different pitch distances

Hoops Spacing	Strain	Stress (Ksi)
6 inches	0.0182	4.7843
7 inches	0.0187	4.5730
8 inches	0.0186	4.3893
9 inches	0.0187	4.2940
10 inches	0.0192	4.1961
11 inches	0.0198	4.0872
12 inches	0.0204	4.0563
Without Hoop	0.0022	0.0050

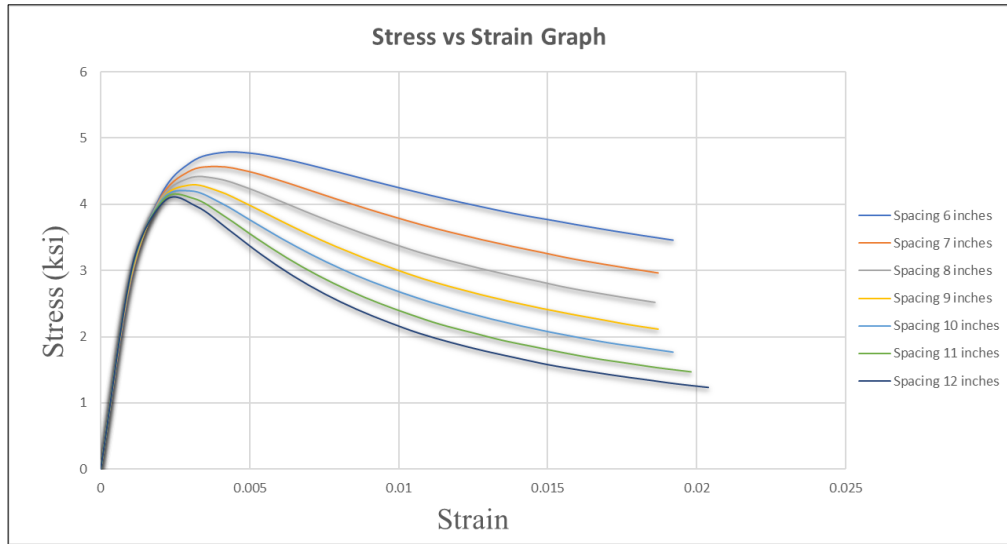


Figure 10. Stress-Strain graph for different pitch conditions

Finding the effective orientation of confinement in reinforced column:

Here for finding the effective confinement orientation in reinforced column there are six different models have been used in Abaqus FE simulation. Each model has significant difference to each other. The difference of the consecutive models has not only in their hoops distance (not necessarily in linear way) but also in their hoops number and orientation, the analytical results are presented in Table 4. and also characterized by Fig. 11.

Table 4. Combined table from the analysis result

Model name	Ultimate Force (kN)	Displacement at Ultimate Force (mm)	Area of Rein. (mm²)	Force/Reinforcement (kN/mm²)
01	4667.718	4.50	851.6112	5.481
02	4541.295	4.65	754.8372	6.016
03	4497.565	4.20	851.6112	5.281
04	4506.795	4.00	851.6112	5.292
05	4737.519	4.70	922.5788	5.135
06	4659.881	4.75	922.5788	5.050

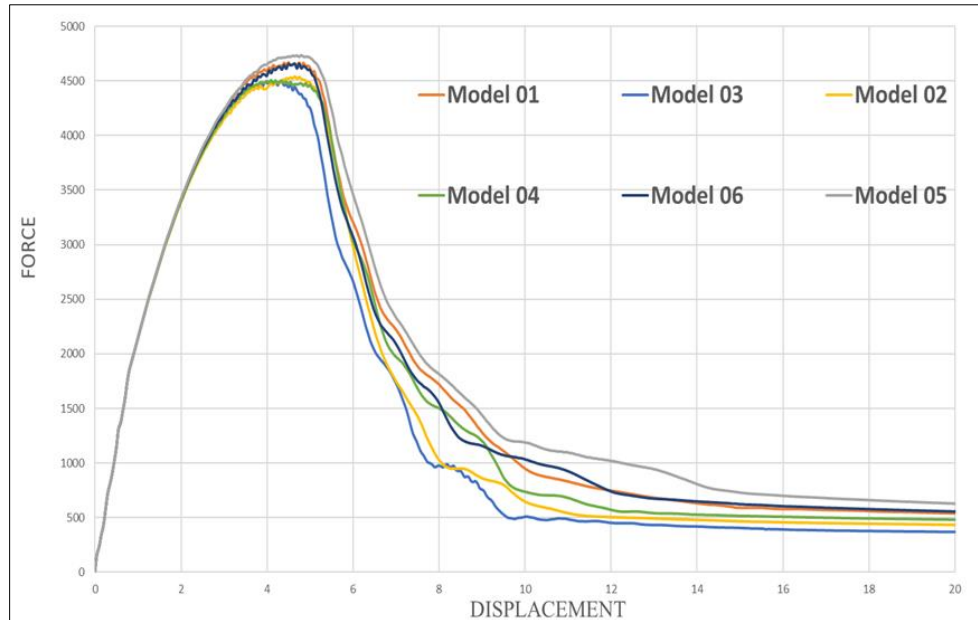


Figure 11. Combined Force vs Displacement graph

Change in reinforcement distribution, with greater spacing in certain regions and increased area in others, may reflect an optimization based on the column's individual load and performance requirements. This improved distribution may result in more efficient load transfer mechanisms and, as a result, larger peak forces per hoop.

Model 02 achieves the highest force-to-reinforcement ratio (6.016 kN/mm^2), indicating the most efficient use of reinforcement material. Although its ultimate force (4541.295 kN) is not the highest, the smaller reinforcement area (754.8372 mm^2) ensures that the material is utilized effectively. This makes Model 02 the most economical choice when balancing structural performance with resource utilization. Model 01 demonstrates the highest ultimate force (4667.718 kN) with low displacement (4.50 mm), showcasing strong load-carrying capacity and minimal deformation. However, its force-to-reinforcement ratio (5.481 kN/mm^2) is lower than Model 02, indicating less efficient material usage. Model 05 delivers the second-highest ultimate force (4737.519 kN) but requires the largest reinforcement area (922.5788 mm^2), resulting in a lower efficiency ratio of 5.135 kN/mm^2 . While it provides strong capacity, it is less economical compared to Model 02. Model 06, with a similar ultimate force, exhibits the highest displacement (4.75 mm) and the lowest force-to-reinforcement ratio (5.050 kN/mm^2), making it less

effective in both performance and material usage. Models 03 and 04 offer moderate performance but are outperformed by Model 02 in efficiency and by Model 01 in strength.

Overall, Model 02 is the most efficient design with the highest force-to-reinforcement ratio (6.016 kN/mm^2), while Model 01 excels in strength for applications prioritizing ultimate load capacity.

The strength and ductility of the column can be improved by adjusting the distribution of reinforcement. While some regions might benefit from greater ductility, others might need more reinforcement to withstand higher loads. Optimization seeks to use materials efficiently, avoiding overdesign in areas where loads are lower. This approach is crucial for economic reasons and sustainability, as it minimizes the use of materials without compromising safety.

To achieve strain compatibility throughout the column, the distribution of reinforcement can be adjusted. It guarantees that the column's various sections deform in unison, encouraging ductile behavior and averting untimely failure.

6 Conclusions

Lateral reinforcement is integral in confining concrete within a column, enhancing both strength and ductility by preventing premature spalling or crushing. This confinement allows the column to deform more ductility before failure and prevents buckling of longitudinal reinforcement (main bars), crucial for maintaining their stability under high axial loads. The study highlights the importance of optimizing reinforcement distribution to improve the strength, ductility, and efficiency of columns. By strategically varying the spacing and area of reinforcement, it is possible to enhance the load transfer mechanisms within the column, allowing it to achieve higher peak forces with better material utilization. Regions subject to higher stresses may require denser reinforcement, while areas experiencing lower stresses can have reduced reinforcement, ensuring a balanced design that avoids overdesign in less critical zones. This approach is not only economical but also promotes sustainability by minimizing material usage without compromising structural safety.

Among the models studied, Model 02 stands out with the highest force-to-reinforcement ratio (6.016 kN/mm^2), indicating the most efficient use of materials. While

its ultimate force (4541.295 kN) is not the highest, its smaller reinforcement area (754.8372 mm²) reflects a well-optimized design. On the other hand, Model 01 demonstrates the highest ultimate force (4667.718 kN) with minimal displacement (4.50 mm), making it ideal for applications where maximum load capacity is critical, albeit at a slightly lower efficiency.

Optimizing reinforcement distribution also ensures strain compatibility across the column, encouraging uniform deformation and ductile behavior. This reduces the risk of premature failure, making the column safer and more reliable under varying load conditions. Increasing the hoops area in the middle zone of a reinforced concrete column positively influences both load-carrying and deformation capacities. This practice enhances the performance of columns where ductility is a critical consideration, allowing for a more economical design by utilizing smaller and cost-effective structural members, thereby reducing material and construction.

Acknowledgements

The Authors would like to thank The Almighty and everyone who supported and contributed to the completion of this work.

References

- [1] D. C. Kent and R. Park, "Flexural Members with Confined Concrete," *Journal of the Structural Division*, vol. 97, no. 7, 1971, doi: 10.1061/jsdeag.0002957.
- [2] E. Hognestad, "A Study of Combined Bending and Axial Load in Reinforced Concrete Members," *Bulletin Series No. 399*, 1951.
- [3] S. Popovics, "A numerical approach to the complete stress-strain curve of concrete," *Cem Concr Res*, vol. 3, no. 5, 1973, doi: 10.1016/0008-8846(73)90096-3.
- [4] A. Thorenfeldt, E. Tomaszewicz and J. Jensen, "Mechanical properties of high-strength concrete and application in design," in *Proceedings of the symposium utilization of high strength concrete*, 1987.
- [5] W. T. Tsai, "Uniaxial Compressional Stress-Strain Relation of Concrete," *Journal of Structural Engineering*, vol. 114, no. 9, 1988, doi: 10.1061/(asce)0733-9445(1988)114:9(2133).

- [6] H. E. H. Roy and M. A. Sozen, “Ductility of Concrete,” *Symposium Paper*, vol. 12, pp. 213–235, Jan. 1965.
- [7] P. Desayi, K. T. Sundara Raja Iyengar, and T. Sanjeeva Reddy, “Equation for stress-strain curve of concrete confined in circular steel spiral,” *Matériaux et Constructions*, vol. 11, no. 5, 1978, doi: 10.1007/BF02473875.
- [8] B. D. Scott, R. Park, and M. J. N. Priestley, “Stress-Strain Behavior of Concrete Confined by Overlapping Hoops at Low And High Strain Rates.,” *Journal of the American Concrete Institute*, vol. 79, no. 1, 1982, doi: 10.14359/10875.
- [9] J. B. Mander, M. J. N. Priestley, and R. Park, “Observed Stress-Strain Behavior of Confined Concrete,” *Journal of Structural Engineering*, vol. 114, no. 8, 1988, doi: 10.1061/(asce)0733-9445(1988)114:8(1827).
- [10] J. B. Mander, M. J. N. Priestley, and R. Park, “Theoretical Stress-Strain Model for Confined Concrete,” *Journal of Structural Engineering*, vol. 114, no. 8, 1988, doi: 10.1061/(asce)0733-9445(1988)114:8(1804).
- [11] K. J. Willam and E. P. Warnke, “Constitutive Model for the Triaxial Behavior of Concrete,” in *IABSE} Proceedings, Vol 19, 1975*.
- [12] G. Schickert and H. Winkler, “Results of test concerning strength and strain of concrete subjected to multi-axial compressive stress,” pp. 123–123, 1977.
- [13] Y. Yong, M. G. Nour, and E. G. Nawy, “Behavior of Laterally Confined High-Strength Concrete under Axial Loads,” *Journal of Structural Engineering*, vol. 114, no. 2, 1988, doi: 10.1061/(asce)0733-9445(1988)114:2(332).
- [14] L. Bjerkeli, A. Tomaszewicz, and J. J. Jensen, “Deformation properties and ductility of high-strength concrete,” in *American Concrete Institute, ACI Special Publication*, 1990. doi: 10.14359/2844.
- [15] L. Bing, R. Park, and H. Tanaka, “Constitutive behavior of high-strength concrete under dynamic loads,” *ACI Struct J*, vol. 97, no. 4, 2000, doi: 10.14359/7427.
- [16] L. Bing, R. Park, and H. Tanaka, “Stress-strain behavior of high-strength concrete confined by ultra-high- and normal-strength transverse reinforcements,” *ACI Struct J*, vol. 98, no. 3, 2001, doi: 10.14359/10228.
- [17] M. Guadagnuolo, A. Donadio, A. Tafuro, and G. Faella, “Experimental Behavior of Concrete Columns Confined by Transverse Reinforcement with Different Details,” *The Open Construction & Building Technology Journal*, vol. 14, no. 1, 2020, doi: 10.2174/1874836802014010250.